De Haas–van Alphen Effect and Fermi Surface in Palladium*

JOSEPH J. VUILLEMIN†‡§
Institute for the Study of Metals and Department of Physics, The University of Chicago, Chicago, Illinois
(Received 24 September 1965)

A detailed study of the de Haas–van Alphen (dHvA) effect in Pd by the field modulation technique is presented. The dHvA oscillations were observed in magnetic fields up to 53 kG at temperatures between 1 and 2°K. Two distinct sets of oscillations were observed with the field in either the (110) or the (100) planes. These are interpreted by a rigid-band model using the known Cu band structure. The oscillations correspond to (1) electrons in the s band and (2) small pockets of holes in one of the d bands. The electron surface is closed and it is centered at Γ. The hole surfaces, also closed, are located at X; and they are approximately ellipsoidal with their major axis along [100]. The electron surface contains 0.36 ± 0.01 electrons/atom while the hole ellipsoids contain only 5.4×10^{-3} holes/atom. The average effective mass $m=2.2m_0$ for the electrons, and the smallest hole mass $m_{100}=(0.63\pm0.05)m_0$. There is also a second d-band hole surface which is open along [100]. The total number of holes is thus 0.36 ± 0.01 per atom, since Pd is a compensated metal. This model also provides a complete interpretation of the galvanomagnetic data. The effects of spin-orbit coupling on the d-band surfaces are discussed in terms of a semiempirical calculation by Mueller. Since the known Cu band structure explains almost every detail of the present experiment, it provides direct evidence that the band structures of certain transition metals have many common features.

I. INTRODUCTION

TRANSITION metals are those for which the Fermi level lies within the d bands.[1] These d bands are relatively narrow and hold 10 electrons per atom so their electronic density of states is typically much larger than that in simple metals. They thus play an important role in the characteristic electrical, magnetic, and optical properties of transition metals. However, a complete understanding of this role has been hindered by a lack of detailed knowledge of the band structures of individual transition metals.

In this paper, the results of a detailed study of the de Haas–van Alphen (dHvA) effect in palladium are presented, and this is shown to yield a great deal of information about its electronic band structure. Palladium is a particularly interesting transition metal because it has an extremely high density of states at the Fermi level, as measured by the electronic specific heat (9.3 mJ deg^{-2} mole^{-1}).[2] The paramagnetic susceptibility is correspondingly large,[3] and a theoretical analysis of its temperature variation has concluded that the d bands contain approximately 0.32 holes/atom.[4] There has also been a series of experiments on alloys of Pd with its neighbors in the periodic table, Rh and Ag (all are fcc). With the assumption of a rigid-band model,[5] these have been used to show that the Fermi level in Pd lies just above a high peak in the density of states and that the d bands contain 0.58 holes/atom.[6] This larger value is usually accepted; but the present measurements yield directly the value 0.36 ± 0.01, although the band structure found is remarkably similar to that for Cu and Ag.

The only other detailed information about the band structure comes from the galvanomagnetic data of Alekseevskii *et al.*[7] These measurements show that part of the Fermi surface of Pd is open and that the open part is topologically equivalent to a spatial network of cylinders with axes directed along the [100] directions. The galvanomagnetic data also verify that Pd is a compensated metal with the number of electrons equal to the number of holes ($n_e=n_h$). This compensation is expected in Pd because outside the filled inner shells there are 10 electrons which must be divided between the s and d bands in the metal. It is shown below that in the light of the present interpretation of the Pd band structure, the galvanomagnetic data give important information about the d bands.

The Fermi surface experiments, of course, yield direct information only about the immediate neighborhood of the Fermi level; but this can often be used to infer the band structure over a much wider energy range.[8–10] One of the most powerful tools for studying the Fermi surface of a metal is the dHvA effect, which is the periodic variation in magnetization with reciprocal field. The dHvA effect can be observed only at low temperatures, and the frequency F of the susceptibility oscillations is related to the extremal cross-sectional area A of the Fermi surface normal to the field by the

* Supported by the National Science Foundation and the Advanced Research Projects Agency.

† Submitted in partial fulfillment of the requirements for the Ph.D. degree at the University of Chicago.

‡ National Science Foundation Predoctoral Fellow.

§ Present address: Royal Society Mond Laboratory, Cambridge University, Cambridge, England.

[1] For a review, see *Advances in Physics*, edited by N. F. Mott (Taylor and Francis Ltd., London, 1964), Vol. 13, p. 325.

[2] F. E. Hoare and B. Yates, Proc. Roy. Soc. (London) **A240**, 42 (1957).

[3] F. E. Hoare and J. C. Matthews, Proc. Roy. Soc. (London) **A212**, 137 (1952).

[4] M. Shimizu, J. Phys. Soc. Japan **15**, 376 (1960).

[5] N. F. Mott, Proc. Roy. Soc. (London) **47**, 571 (1935).

[6] D. W. Budworth, F. E. Hoare, and J. Preston, Proc. Roy. Soc. (London) **A257**, 250 (1960).

[7] N. E. Alekseevskii, G. E. Karstens, and V. V. Mozhaev, Zh. Eksperim. i Teor. Fiz. **46**, 1976 (1964) [English transl.: Soviet Phys.—JETP **19**, 1333 (1964)].

[8] N. W. Ashcroft, Phil. Mag. **8**, 2055 (1963).

[9] J. R. Anderson and A. V. Gold, Phys. Rev. **139**, A1459 (1965).

[10] F. Mueller (to be published).

Onsager expression,[11]

$$A=4\pi^2eF/h=2.673\times10^{-9}F. \quad (1)$$

The area A in $\mathbf{k}$ space is in atomic units (a.u.) when F is in gauss.

The first observation of the dHvA effect in Pd was made by the pulsed-field technique.[12] Preliminary results[13] with the field-modulation technique (discussed in Sec. II) showed that the Fermi surface of Pd was consistent with a band structure like that of Cu, with the Pd Fermi level displaced to just below the top of the d bands. The results of a much more comprehensive and accurate study of the dHvA effect by the field-modulation technique are presented in Sec. III. The observed surfaces are attributed to electrons in the s band and to holes in one of the d bands. The results are discussed in Sec. IV in the light of recent semiempirical band calculations for Pd which include the effects of spin-orbit coupling in the d bands.[10] The surfaces observed by the dHvA effect are closed, and it is deduced that the open surface found in the galvanomagnetic experiment[7] represents the other d-band surface. By combining the results of the dHvA study with the galvanomagnetic data, a rather complete and self-consistent picture of the Fermi surface and the band structure near the Fermi level is obtained. The resulting band structure for Pd is used in Sec. V to interpret the alloy data. The application of this rigid-band model to other fcc transition metals is also discussed.

II. EXPERIMENTAL TECHNIQUES

The dHvA oscillations were observed by means of a modulation technique similar to that developed by Shoenberg and Stiles.[14] In this technique, the sample is surrounded by a pickup coil and placed in a high dc field $\mathbf{H}$ upon which a modulating field of the form $\mathbf{h}\cos\omega t$ is superimposed. The emf induced in the pickup coil contains harmonics of the modulating frequency because the sample magnetization is a nonlinear function of H. The amplitude of each harmonic component is proportional to the oscillatory part of the magnetization.

In this experiment, phase sensitive detection of the signal developed across the pickup coil was employed. The detector was driven at the second harmonic frequency 2ω and its output was a dc signal proportional to the amplitude of the second harmonic signal. Oscillations in the magnetization, such as those shown in Fig. 3, were plotted directly from the detector output with an X-Y recorder.

The modulation amplitude h needed for second harmonic detection is of the same order of magnitude as the spacing in H of the dHvA oscillations. This spacing is given by $\delta H=H^2/F$ where F is the dHvA frequency. Two sets of oscillations were observed: one due to electrons with $F\geqslant2.5\times10^8$ G, and the other due to holes with $F\leqslant0.9\times10^7$ G. Therefore, these two sets of oscillations required modulating fields of the order of 10 and 100 G, respectively, for H in the range 30 to 50 kG.

Modulation frequencies of 100, 600, and 2200 cps were used. The 100 cps frequency was used where the larger modulation fields were applied. When the larger modulating currents were applied at 600 cps and higher, mechanical vibrations were excited making the signal-to-noise ratio somewhat worse than that at 100 cps. Where the smaller modulation fields were used, the 600 cps modulating frequency gave about the optimum signal-to-noise ratio. Although the rate of change of flux within the pickup coil is greater at the higher frequencies, the magnitude of the dHvA signal will be affected by the skin effect. The second harmonic signal is generated below the sample surface, and the signal will be partially shielded from the pickup coil if the second harmonic skin depth is less than the sample radius. The skin depth in Pd at 45 kG is equal to the sample radius (0.5 mm) when the frequency is about 1.6 kc assuming a residual resistance ratio of 4000 and $\Delta\rho/\rho_0=50$ ($\sigma=6\times10^6$ mho cm^{-1}).[7]

The field $\mathbf{H}$ was supplied by a 53-kG Varian superconducting solenoid which operated in a liquid-He bath at 4.2°K. The bore of the solenoid was 1.03 in., and the 1-in.-diam tail of a second He Dewar was fitted inside the solenoid. The sample, the balanced pickup coil, and the modulation coil were mounted in a $\frac{3}{4}$-in.-diam epoxy gear wheel which was inserted into the inner Dewar tail. The gear wheel could be rotated about a horizontal axis by means of a second epoxy spiral gear[15] which was turned from the top of the cryostat. This rotating mechanism which could easily be calibrated in air and in liquid He (see Sec. III) allowed the sample to be oriented with respect to the field over a 180° range with an accuracy of approximately 0.3°. Temperatures as low as 0.95°K were reached by pumping on the liquid He in the inner Dewar. These were measured by a 33 Ω Allen Bradley carbon resistor which was calibrated from He vapor pressure measurements.

The superconducting solenoid had been corrected for field inhomogeneities to the sixth order.[16] The measured inhomogeneity was about 2 parts in 10^5 at 38 kG over 1 cm. A Na^{23} NMR probe was used to determine the homogeneity and the current calibration of the solenoid. During the experiments, the solenoid field strength was measured by means of an air cooled manganin 0.1252 Ω resistor in series with the solenoid. At maximum current (15 A), the temperature rise of this resistor was less than 20°C, and the corresponding change in resistance

[11] L. Onsager, Phil. Mag. **43**, 1006 (1952).
[12] J. J. Vuillemin and M. G. Priestley, Bull. Am. Phys. Soc. **9**, 632 (1964).
[13] J. J. Vuillemin and M. G. Priestley, Phys. Rev. Letters **14**, 307 (1965).
[14] D. Shoenberg and P. J. Stiles, Proc. Roy. Soc. (London) **A281**, 62 (1964).
[15] A. C. Thorsen and T. G. Berlincourt, Rev. Sci. Instr. **34**, 435 (1962).
[16] M. W. Garrett, J. Appl. Phys. **22**, 1091 (1951).

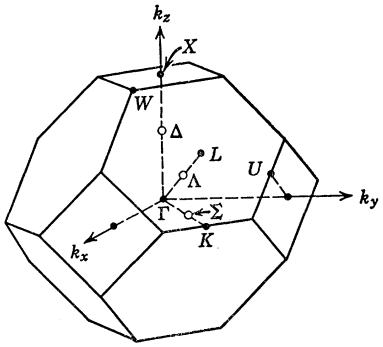

FIG. 1. The first Brillouin zone for a fcc lattice such as that of Pd. The standard notation is used.

was less than 1 part in 10^4. It should be noted that the field measurements used in a preliminary publication[13] were uniformly 1% high because of an error in the location of the current resistor.

Since the spacing in H of the dHvA oscillations is of the order of 10 G, it is necessary to sweep only a small portion (ΔH) of the field in order to observe 100 oscillations. In order to display only ΔH on the X axis of the recorder, a Princeton voltage reference source, model CT602CR, was used to apply a backoff voltage to the current sampling resistor. The difference between the backoff voltage and the voltage developed across the resistor was used to produce the X deflection on the recorder. In this manner, the absolute solenoid current could be measured accurately to 1 part in 10^4 and the incremental current to 1 part in 10^3. The corresponding field was not, however, determined so accurately because of flux jumps which occurred within the solenoid turns.[17] Apparently, this behavior is characteristic of most superconducting solenoids. Field measurements with the NMR probe indicated that the current calibration of the solenoid could fluctuate by as much as 0.1% at 35 kG depending on the previous history of the solenoid. Since this fluctuation could occur during a field sweep, the error in ΔH was rather greater than this, and it occasionally reached 0.5%. For this reason, the dHvA frequency measurements were limited to 0.5% accuracy. The pulsed field data[12] provide an independent set of dHvA frequency measurements to compare with the present results. These two sets of data are in good agreement although the pulsed-field data were only accurate to 2%. Pulsed-field measurements were not made in great detail because much higher sensitivity was found with the field-modulation technique.

Single-crystal specimens of high purity were obtained from zone-refined rods of Pd. Johnson-Matthey's spectroscopically standardized (JM942) 1-mm Pd wire was used for raw material. According to the manufacturer, the total metallic impurity content was less than 10 parts per million (ppm) with the major impurities estimated to be: Fe (2 ppm), Si (2 ppm), and Ca (1 ppm).

The 1-mm rods were zone refined by the floating-zone technique. Several passes at a speed of $\frac{1}{2}$ in./h were made on each rod. Zone refining was carried out under one atmosphere of argon, and the rod was melted by induction heating. The 450-kc energy, which had been carefully stabilized against line-frequency ripple, was transferred to the 1-mm Pd rod by means of a water-cooled copper concentrator.[18] The molten zone in these small diameter rods was very stable. It is thought that the molten zone was inherently stable because of the conditions of power transfer. Provided the skin depth is greater than the rod diameter, the increased resistivity on melting causes the power transferred to the rod to decrease.[19]

Without seeding, several single crystals about 1 in. in length were obtained with either a [110] or a [100] axis nearly perpendicular to the rod axis. Rods approximately 4 mm in length were spark cut from the 1-mm-diam single crystals and mounted in loose fitting epoxy cylinders with a dot of glue. Data for the specimens from which results are quoted in this paper are listed in

TABLE I. Palladium sample data. The angles ζ and ξ are the polar and azimuthal angles, respectively, of the specimen axis relative to the [100] crystal axes. The resistivity is given by ρ. Pd II was used only with pulsed fields.

Sample No.	Orientation ζ^0	Orientation ξ^0	$\rho(300°K)/\rho(4.2°K)$
II	40	45	6500
IX	40	46	4000
IXA	38	48	4000
X	77	2	4800

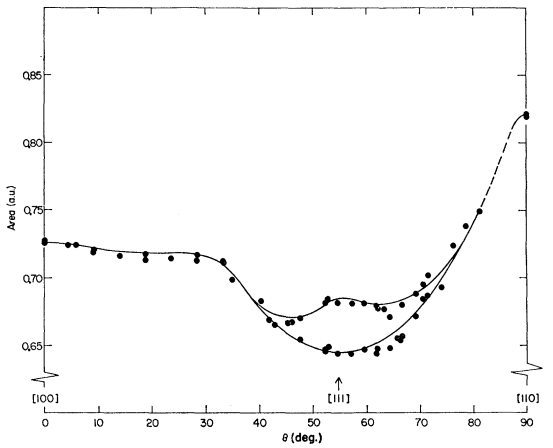

FIG. 2. The measured extremal cross-sectional area of the electron Fermi surface with **H** in a (110) plane for Pd IX. The solid line represents the measured variation in the area by field rotation with $A_{100}=0.726$ a.u. while the data points are from field sweeps. Over the dashed region the amplitude of the oscillations was very small and there were more than 60 per degree so a continuous rotation pattern could not be obtained.

[17] C. H. Rosner, J. Appl. Phys. **36**, 1175 (1965).

[18] R. W. Johnson, J. Appl. Phys. **34**, 352 (1963).

[19] N. R. Stansel, *Induction Heating* (McGraw-Hill Book Company, Inc., New York, 1949).

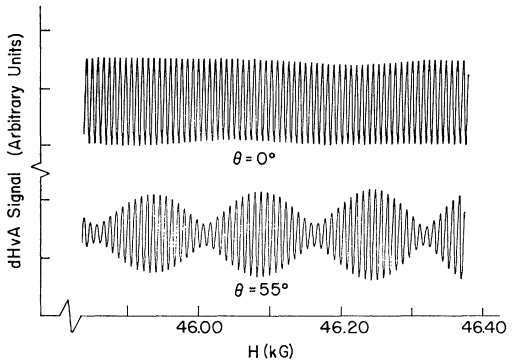

FIG. 3. Oscillations in the magnetization due to the electron surface for Pd IX with **H** near [111], $\theta=55°$, and [100], $\theta=0°$, and $T=1.0°$K. The lower curve shows the beats observed near [111] which give rise to the double values of area.

Table I. An indication of the purity of the specimens is given by the residual resistance ratio. The orientation of the specimen axes were determined with an accuracy of 0.5° from Laue back reflection x-ray photographs.

III. RESULTS

Palladium is a fcc metal whose Brillouin zone is the polyhedron shown in Fig. 1. Because of the high symmetry of this zone, a rather complete picture of the Fermi surface can be obtained from measurements of the extremal cross-sectional area when the field is tipped in the (110) and (100) planes. Two distinct sets of areas were observed in these planes. Since the frequencies of the electron and the hole oscillations were separated by more than an order of magnitude, there was no interference between the two sets of oscillations. For reasons which are given in Sec. IV, the set of larger areas is attributed to electrons and the smaller to holes.

Under the present experimental conditions, the observed component of the oscillatory magnetization has the form[20]

$$M_{\rm osc}\propto a(\mathbf{H})\sin[\hbar A/(eH)\pm\pi/4-2\pi\gamma], \qquad (2)$$

where A is the extremal cross-sectional area of the Fermi surface normal to the field **H**, $a(\mathbf{H})$ is a slowly varying function of **H**, and γ depends only on the energy dispersion law ($\gamma=\frac{1}{2}$ for a quadratic law). Oscillations were observed in two ways: either (1) by changing $|\mathbf{H}|$ keeping its direction constant, or (2) by changing A (the Fermi surface was not isotropic) by rotating **H** with $|\mathbf{H}|$ constant.[14] Absolute area measurements were obtained by the former method, while the latter gave only differential measurements of area. The field rotation method was the more accurate because $\hbar A/e\gg H$.

[20] I. M. Lifshitz and A. M. Kosevich, Zh. Eksperim. i Teor. Fiz. **29**, 730 (1955) [English transl.: Soviet Phys.—JETP **2**, 636 (1956)].

A. The Electron Surface

Figure 2 shows the electron surface cross-sectional area as a function of the angle θ between **H** and [100] with **H** in a (110) plane. Oscillations were observed throughout the (110) plane, and therefore the surface is closed. The electron surface is centered at Γ in the Brillouin zone (see Fig. 1) because the area is single valued for most field directions (see Figs. 2 and 8). However, when the field is near [111], the oscillations show the beating of two frequencies as in Fig. 3. The separation in the double values of the area near [111] was obtained from the observed beat frequencies. The variation of the area in the (110) plane shows that the electron surface has bumps along the [111] directions, and consequently the double values for **H** near [111] are associated with (1) a central section containing Γ and (2) two equivalent noncentral sections passing over the [111] bumps. There are also smaller bumps at [100] because $A_{111}<A_{100}<A_{110}$.

The solid line in Fig. 2 represents the variation in area as measured by the field-rotation method described above with $A_{100}=0.726$ a.u. Oscillations in the magnetization observed when the field was rotated slowly through [100] in a (110) plane are shown in Fig. 4. The change in area is given by

$$A_{100}-A=\pm 2.673\times 10^{-9}nH, \qquad (3)$$

where the area A is in a.u. if H is in gauss, and where n is the number of oscillations from [100]. The sign of the area change can be determined from the absolute measurements. Each oscillation in Fig. 4 corresponds to a difference in area of about 2 parts in 10^4 of A_{100}. As it is shown in Fig. 4, the symmetry directions can be accurately located by the field-rotation method. This method proved to be the most accurate way of calibrating the angular scale. The room-temperature measurements also agreed with this calibration.

The differential area measurements in the (110) plane are shown in Figs. 5 and 6. The smooth curve is a part of that shown in Fig. 2. The error in the differential

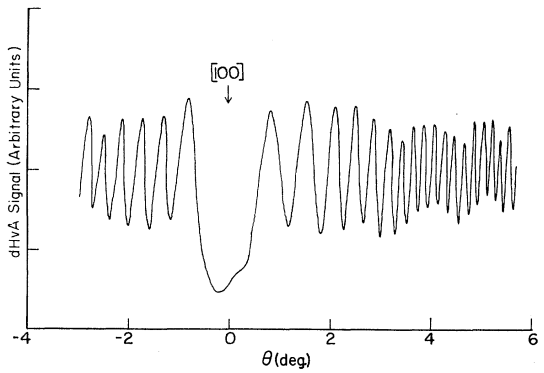

FIG. 4. Field rotation for Pd IX, with **H** in a (110) plane. $H=45.6$ kG and $\dot{\theta}=1°$/min. Each oscillation corresponds to a change in area of about 2 parts in 10^4.

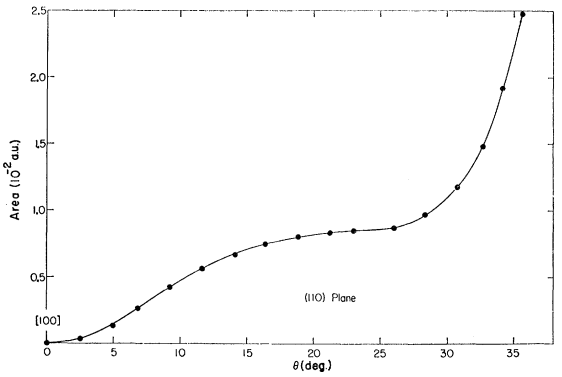

FIG. 5. Relative electron surface area measurements for Pd IX with **H** in a (110) plane. The smooth curve was drawn through the data points obtained from a rotation diagram.

measurements in Fig. 5 is a few parts in 10^4 of A_{100}, while that in Fig. 6 is approximately one part in 10^3 of A_{100}. This reduction in accuracy came about because it was difficult to distinguish two sets of oscillations by the field rotation method over a small part of the double-valued region. The variation in the noncentral section (lower curve in Fig. 6) was determined by combining the field rotation and the beat frequency measurements. The curves shown in Fig. 6 are consistent with both types of measurements.

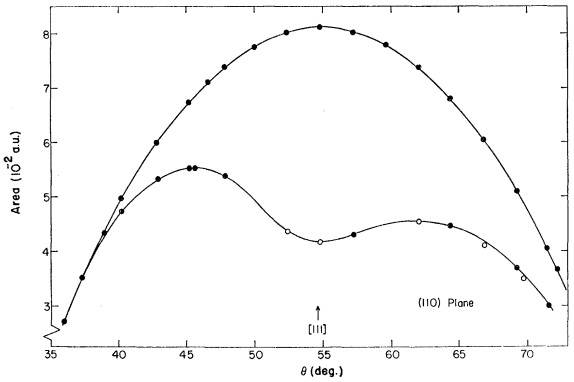

FIG. 6. Relative electron-surface area measurements for Pd IX with **H** in a (110) plane in a region where the extremal area is double valued. The open circles were obtained from the beat frequency in a field sweep and the solid circles from a field rotation.

Figure 7 shows the observed oscillations in the magnetization when the field was rotated in the (110) plane. Note that two sets of oscillations are present over the angular range shown, except near $\theta=47°$. The slower oscillation belongs to the noncentral section which has a stationary value at $\theta=45.5°$ (see Fig. 6).

Figure 8 shows the cross-sectional area measurements with **H** in the (100) plane. The three stationary values near [100] were evident only in field-rotation plots since the variation over these values is only 0.5% of A_{100}. These field rotation measurements are shown in the inset in Fig. 8. The maximum in the area at [110] and the local maximum at [100] are consistent with the previously discussed electron surface.

In order to estimate the radii at the symmetry directions and the volume of the electron surface, an empirical interpolation scheme was devised. The empirical surface consists of a sphere upon which axially symmetric bumps with sinusoidal cross sections are superimposed in the [100] and [111] directions. This model satisfies the crystal symmetry and it is analytically integrable. The radial coordinate in the neighborhood of a bump has the form

$$k=k_0+\Delta k[1+\cos(\pi\alpha/\alpha_0)]. \quad (4)$$

As it is shown in Fig. 9, k_0 is the radius of the sphere

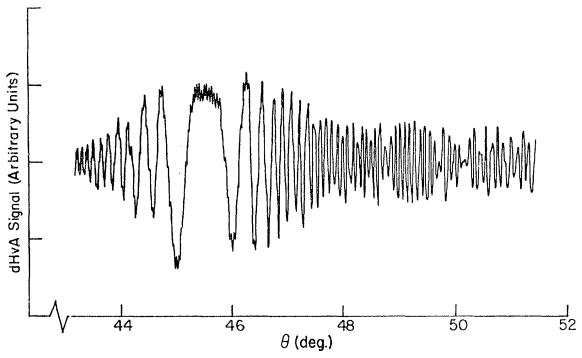

FIG. 7. A field rotation plot of the dHvA signal for Pd IX with **H** in a (110) plane. The angle between **H** and [100] is given by θ, and $H=46.2$ kG. Note that two oscillations are present.

upon which the bumps are superimposed, $2\Delta k$ is the bump height, α is the angle between **k** and the axis of the bump, and α_0 is the angular half-width of the bump. The best fit for the empirical surface was obtained with the parameters given in Table II. The resulting (100) and (110) sections of this surface are shown in Fig. 10. Although the area measurements were accurate to 1%,

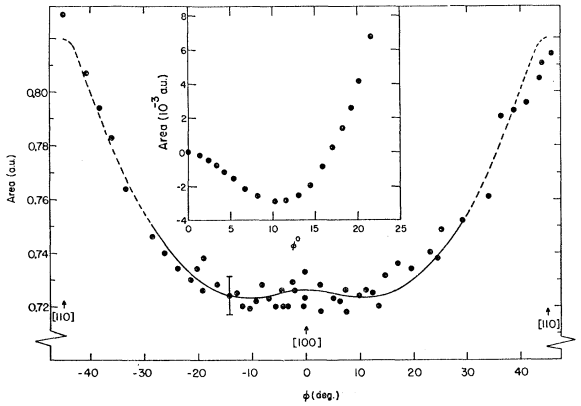

FIG. 8. The measured extremal cross-sectional area of the electron Fermi surface for Pd X with **H** directed in a (100) plane. The solid line was obtained from a field rotation using $A_{100}=0.726$ a.u. The inset shows the measured variation near [100] on an expanded scale.

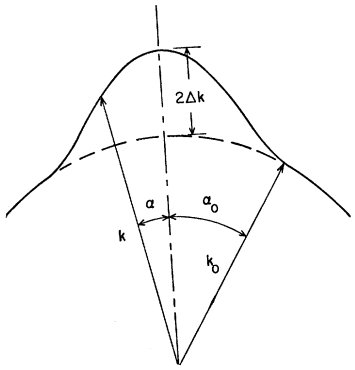

FIG. 9. Schematic representation of the empirical electron surface parameters. The bumps are super-imposed on a sphere of radius k_0 and are axially schematic.

the radii are probably in error by as much as 6%. The volume of the fitted surface in **k** space, consisting of the sphere and the bumps, was found to be 0.36±0.01 electrons/atom. This volume is in agreement with that of a sphere whose cross-sectional area is equal to the average of the measured areas in the (110) plane.

B. The Hole Surface

The observed hole surfaces are approximately surfaces of revolution obtained by rotating an ellipse about its major axis. Figure 11 shows the area measurements

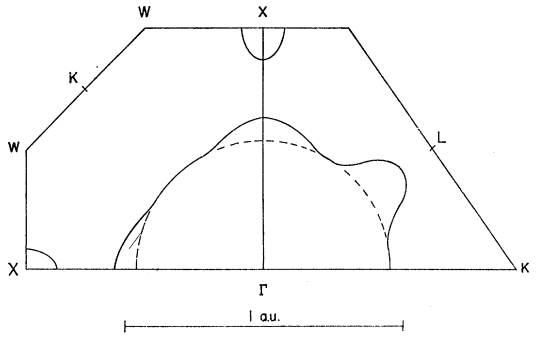

FIG. 10. The (100) and (110) sections of the empirically determined electron surface and hole ellipsoids for Pd. The dimensions of the electron surface are given in Table II.

for the hole surfaces with **H** in a (110) plane. In this figure, the solid lines are an ellipsoidal fit to the data with the major axes of the ellipsoids along [100]. The best fit was obtained with the semimajor and the semi-minor axis of each ellipsoid of revolution equal to 0.113 a.u. and 0.070 a.u., respectively. Each ellipsoid occupies a volume in **k** space of only 1.8×10^{-3} holes/atom. The area measurements in the (100) plane with the same ellipsoidal fit used for the (110) data are shown in Fig. 12.

Since the smaller central sections of the ellipsoids fit the area data quite well up to 60° away from [100], the hole surface deviates from an ellipsoid only at its ends. The deviation is a maximum for the larger [100] area (see Figs. 11 and 12), but this difference cannot

TABLE II. The empirical electron-surface parameters used to fit the area measurements in palladium. The radial coordinate is given by k, the bump height by $2\Delta k$, and the angular half-width of a bump by α_0. These parameters were adjusted to give the [100], the [211], and the central [111] measured areas. The calculated value of $A_{110}=0.81$ a.u.

Orientation	$2\Delta k$ (a.u.)	α_0 (deg)	k (a.u.)
100	0.09	30	0.54
111	0.14	20	0.59
110			0.45
211			0.45

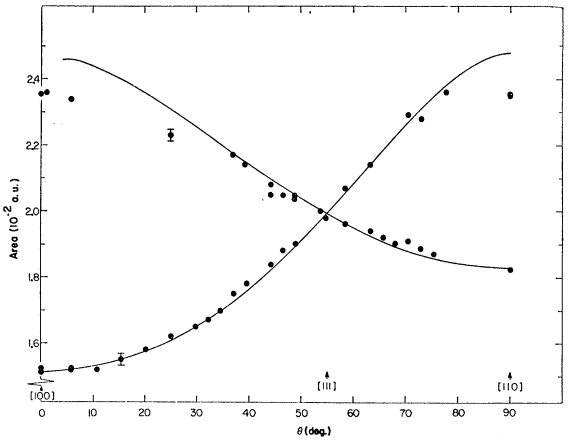

FIG. 11. The measured extremal cross-sectional areas of the hole Fermi surface for Pd IX with the field in the (110) plane. The solid lines are from [100] ellipsoids with $a_1=a_2=0.070$ and $b=0.113$ in a.u.

be ascribed to experimental error in the data. The relevant data are shown in Fig. 13. Since two [100] oscillations are superimposed, the ratio of their frequencies can be accurately determined. If the ellipsoids were truncated to about 80% of their original length, their principal cross-sectional area would agree with the [100] data.

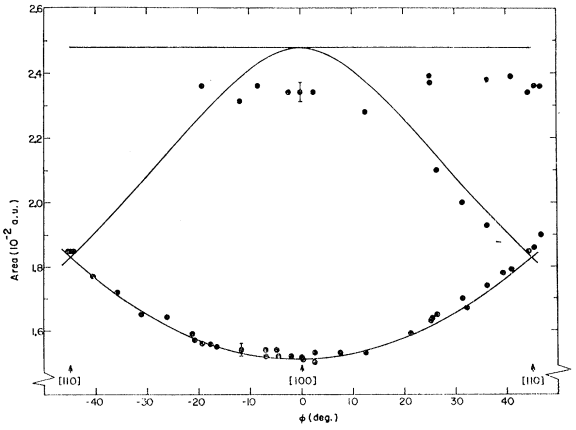

FIG. 12. The measured extremal cross-sectional areas of the hole Fermi surface for Pd X with the field directed in the (100) plane. The solid lines are from the same [100] ellipsoids used to fit the data in Fig. 11.

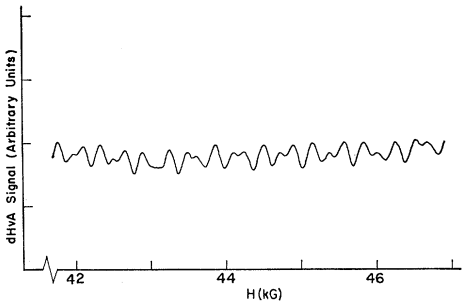

FIG. 13. The oscillations in magnetization due to holes for Pd IX with the field **H** parallel to [100].

The symmetry observed in the hole areas is consistent with that of the points Δ, X, and W in the Brillouin zone (see Fig. 1). However, the point X is preferred on the basis of the band structure presented in Sec. IV. Such a band structure requires the ellipsoids to be holes at the top of the d bands. Since X is the center of a square face, the ellipsoids are repeated three times in the zone, and hence the total observed volume is 5.4×10^{-3} holes/atom. The (110) and (100) sections of the hole surface, as fitted by the ellipsoids, are shown in Fig. 10.

C. The Effective Masses

When $2\pi^2mk_BT/(e\hbar H)\gtrsim 1$, the temperature dependence of the oscillatory magnetization has the form[20]

$$M_{\rm osc}\propto T\exp[-2\pi^2mk_BT/(e\hbar H)], \tag{5}$$

where T is the absolute temperature, k_B is Boltzmann's constant, and m is the cyclotron effective mass. Since the term in the exponent was always greater than 5, this form was expected and observed. The effective mass m is given by

$$m=\frac{\hbar^2}{2\pi}\frac{dA}{d\epsilon}, \tag{6}$$

where the derivative is taken at the Fermi energy.

Figure 14 shows a conventional plot from which the effective mass at a given field direction was obtained.

TABLE III. The effective-mass values for Pd expressed in units of the free-electron mass. The mass m is measured while m (ellipsoid) is proportional to the fitted ellipsoid area with the [100] ellipsoidal mass set equal to m_{100}.

Orientation of **H**	m/m_0	m/m_0 (ellipsoidal)
	holes	
100	0.63±0.05	0.63
	...	1.03
111	0.91±0.09	0.83
110	0.88±0.09	0.77
	...	1.03
	electrons	
100	2.1±0.1	
111	2.3±0.1	

The effective-mass measurements expressed in units of the free electron mass are given in Table III. As it is shown in this table, the variation of the observed hole masses is in agreement with that of an ellipsoidal model.

The field dependence of the amplitude of the de Haas–van Alphen oscillations was not studied because the penetration depth at the second harmonic of the modulating frequency varies with the field H and the dependence of the amplitude on this penetration depth is very complex.

The Fermi energy ϵ_F of the hole surface may be determined now that its effective mass is known. In an ellipsoidal parabolic approximation,

$$\epsilon_F=\hbar^2k_{100}^2/(2m_{100})=7.7\times10^{-3}\ \text{Ry}. \tag{7}$$

The [100] values of k and m were used because they are accurately known.

IV. INTERPRETATION OF THE DATA

A. Band Structure without Spin-Orbit Coupling

The results discussed in the previous section are interpreted as in the preliminary report[13] in terms of a rigid-band model. This is justified by its success in accounting for the observed Fermi surface of Pd; there are no complete and independent Pd band structure calculations, although the d bands have been treated by Friedel *et al.*[21] The Ag band structure is the evident choice for a comparison, but the relative positions of the s and d bands in the Ag calculations[22] do not agree with experiment. The Cu band structure calculations of either Segall[23] or Burdick,[24] on the other hand, are known to be in good agreement with a wide variety of

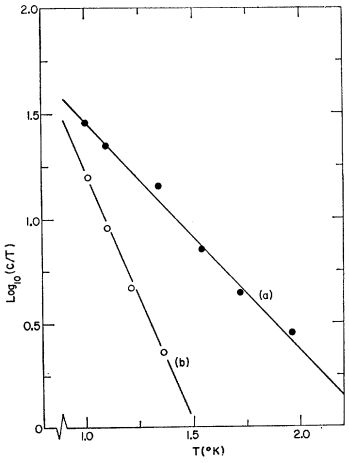

FIG. 14. The temperature dependence of the dHvA amplitude c at H[100] for Pd X. The line (a) is for hole oscillations with $H=37.5$ kG, and (b) is for electron oscillations with $H=42.9$ kG.

[21] J. Friedel, P. Lenglart, and G. Leman, J. Phys. Chem. Solids **25**, 781 (1964).
[22] B. Segall, General Electric Research Laboratory Report No-61RL-(2785G), 1961 (unpublished).
[23] B. Segall, Phys. Rev. **125**, 109 (1962).
[24] G. A. Burdick, Phys. Rev. **129**, 138 (1963).

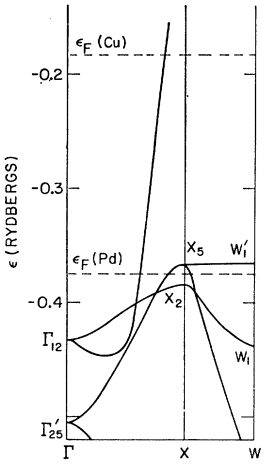

FIG. 15. That part of Segall's Cu band structure (Ref. 23) which is relevant to the interpretation of the Pd data. The zero of energy for Pd is arbitrary.

experiments[25–27] and therefore the Cu band structure was used as a model.

The Cu bands relevant to the interpretation of the Pd Fermi surface are shown in Fig. 15. Since Pd contains one electron less than Cu outside the filled inner shells, the Pd Fermi level will certainly lie lower in the conduction band. Given this band structure, the observed small pieces of Fermi surface find a natural interpretation as holes located at X if the Pd Fermi level ϵ_F(Pd) is placed just below the top of the d bands at X_5. This position of the Fermi level evidently also provides an explanation for the larger piece of surface as electrons in an s band. The magnitude of $X_5-\epsilon_F$(Pd) is determined experimentally as the Fermi energy of the holes. As shown in Sec. IV, this energy is 7.7×10^{-3} Ry in a parabolic approximation. Any error due to the parabolic approximation is relatively unimportant in locating ϵ_F(Pd) with respect to the d bands because the energy $X_5-\epsilon_F$(Pd) is so small compared to the width of a typical Cu band.

It is interesting to note that recent density-of-states calculations made by Mueller[10] have shown that the Cu d bands will contain almost exactly 10 conduction electrons below the Pd Fermi level given in Fig. 15. These density-of-states calculations were made from Burdick's Cu band structure[24] with the aid of an interpolation scheme which permitted accurate determination of the energy (±0.005 Ry) at many more points in the Brillouin zone (approximately 5000 points in 1/48 of the zone) than in previous calculations. Therefore, the Pd Fermi level shown in Fig. 15 is thought to be an accurate estimate of the Fermi energy within the framework of this model.

It now remains to discuss the detailed shape of the s- and d-band surfaces. The s-band surface is closed and it is centered at Γ. The anisotropy of this surface is in good agreement with that of the larger observed surface as shown in Table IV. The magnitude of the radius vector of these two surfaces is also very similar. The detailed discussion of the anisotropy of the small pocket of d-band holes will be deferred until the spin-orbit coupled band structure is considered (Sec. IVB). It is worth noting here, however, that the d band pocket of holes at X_5 in the previously discussed Cu band structure has about the correct anisotropy and volume to fit the data.

The X_5 level is doubly degenerate and so there is another d-band surface at X, i.e., X_5W_1'. In the complete band structure, the corresponding L and U levels lie below ϵ_F(Pd), and therefore the second d-band surface is open. Indeed, this d-band surface is seen to support open orbits in just those directions necessary to explain the galvanomagnetic data[7]; i.e., this surface is topologically equivalent to a network of [100] cylinders. Alekseevskii *et al.*[7] also measured the Hall coefficient for H_{100}. This measurement gives two further important pieces of information: (1) the positive sign of the Hall coefficient shows conclusively that the open surface contains holes, as is also indicated by the previously discussed model; and (2) the magnitude of the Hall coefficient gives an estimate of the size of the necks which does not conflict with this model.

When the data for the surfaces observed in the present experiment are used to calculate their contribution to the electronic specific heat, they account for only approximately 10% of the observed density of states. This implies that the average effective mass of the open d-band surface is very high (~10). If this effective mass is so large, it is immediately clear that this surface cannot be observed by the dHvA effect at 1°K and 50 kG because the Landau level separation is still less than kT.

B. Band Structure with Spin-Orbit Coupling

The interpretation of the results with the spin-orbit coupled band structure is much the same as that for the uncoupled case, except for details at the top of the d bands. Spin-orbit coupling in the d bands of Pd is an important consideration because the corresponding

TABLE IV. Comparison of Fermi surface anisotropy of s- and d-band surfaces (b.s.) with experiment. The average heavy hole neck radius is given by k_{neck}.

Direction of **k**	Electrons k/k_{110} b.s.	exp.	Holes k/k_{100} b.s.	exp.
111	1.37	1.31		
100	1.21	1.20	1.00	1.00
			1.52	1.61
110	1.00	1.00	1.33	1.20
		b.s.	exp.	
Heavy holes: k_{neck}		0.17 a.u.	0.18 a.u.[a]	

[a] Taken from Ref. 7.

[25] S. Roberts, Phys. Rev. **118**, 1509 (1960).
[26] D. Shoenberg and D. J. Roaf, Phil. Trans. Roy. Soc. (London) **255**, 85 (1962).
[27] R. W. Morse, A. Meyers, and C. T. Walker, J. Acoust. Soc. Am. **33**, 699 (1961).

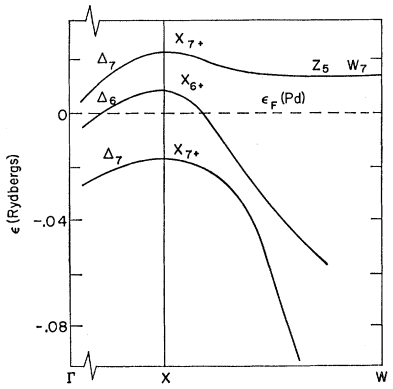

FIG. 16. A portion of the semiempirical d-band structure for Pd as calculated by Mueller (Ref. 10).

splitting in the free atom is the same order of magnitude as the d-band Fermi energy $[X_5-\epsilon_F(\mathrm{Pd})]$ discussed above. In the free atom, $^2D_{3/2}-^2D_{5/2}=3539$ cm^{-1} $=3.2\times10^{-2}$ Ry.[21]

Recent calculations by Mueller based on the same interpolation scheme mentioned above have provided a semiempirical d-band structure for Pd which includes spin-orbit coupling. This structure was obtained from Burdick's Cu band structure[24] by (1) widening the d bands by a factor of 1.5 and (2) applying Pd spin-orbit coupling to the widened d bands. The resulting band structure is shown in Fig. 16. The Fermi energy of the lighter d-band holes is still 7.7×10^{-3} Ry but now this is measured from X_{6+}. The widening of the d bands changed the curvature slightly at the top of these bands and the amount was adjusted so that the effective mass along [100] would agree with the data. The anisotropy of the d bands, however, is not dependent on the widening; and it is in good agreement with observed ellipsoidal surface as shown in Table IV.

The possibility of the Pd Fermi level either lying just below the lower X_{7+} level or above the X_{6+} level is certainly excluded. The effective mass at X_{7+} is almost an order of magnitude higher than that observed and the anisotropy is not correct for the ellipsoids. On the other hand, if the Fermi level were placed 7.7×10^{-3} Ry below the upper X_{7+} level, many contradictions with experiment would appear. In particular, the band structure could no longer support open orbits along [100].

Now that the Pd Fermi level is below X_{6+} as in Fig. 16, the heavy open surface is evidently due to the band $\Delta_7X_{7+}Z_5$. As in the uncoupled case (Sec. IVA), this band structure supports open orbits in just the directions necessary to fit the galvanomagnetic data. The average neck radius (around XW) is in surprisingly good agreement with that of the galvanomagnetic data (see Table IV). The Fermi level relative to the s band has been shifted somewhat from its position in the uncoupled structure, and therefore the s band must be lowered relative to the d bands approximately 0.006 Ry in order for the s-band radii to agree with experiment again.

V. CONCLUSIONS

The Fermi surface of Pd consists of three distinct parts: an electron surface and two sets of hole surfaces. The electron surface is due to the s conduction band, is closed, and is centered on Γ in the Brillouin zone. The shape is approximately that of a sphere, with bumps along [111] and [100]. The radius of this surface varies from 0.45 along [110] to 0.59 a.u. at [111], $\Gamma L=0.744$ a.u. Its volume is 0.36 ± 0.01 electrons/atom, and the average effective mass $m=2.2m_0$.

The smaller of the hole surfaces is approximately ellipsoidal with $a_1=a_2=0.070$ a.u., $b=0.113$ a.u., and the smaller $m_{100}=0.63m_0$. This is due to one of the d bands and there are three surfaces per zone. Their total volume is 5.4×10^{-3} holes/atom. Both these surfaces and the electrons were observed in the dHvA effect, while the remaining hole surface was observed in galvanomagnetic experiments.[7]

The second-hole surface also due to d bands is open, being topologically equivalent to a spatial network of cylinders with axes along [100]. The cylinders intersect at X and their average neck radius is approximately 0.18 a.u. as shown in the galvanomagnetic data. Since Pd is a compensated metal, the total number of holes must be 0.36 ± 0.01 holes/atom. Practically all of the holes then are contained in this surface. The effective mass of this surface must be very high (~10) in order to account for the specific-heat density of states.

Although the rigid-band model has been used extensively for approximately 30 years, the evidence for its validity has remained qualitative and rather indirect in that the details of the band structure were seldom known. Recent calculations and experiments have made the form of the bands much clearer especially for Ni [28,29] and Cu.[24] The Cu band structure[23] is now well established, and nonmagnetic Ni is calculated to have a form very similar to that of the Cu band structure. Ferromagnetic Ni is more complicated, but Phillips has deduced a detailed band structure for the available evidence.[30] As it is shown above, Pd also fits into this rigid-band model since the Cu band structure accounts for all of the data. The correlation appears to extend to the other fcc transition metals Rh [31] and Pt.[32] It seems reasonable then that this same model will apply to the binary alloys of transition and noble metals. However, one would not expect this correlation to apply far from the top right-hand corner of the transition metal group in the periodic table because of the systematic variation in d-band widths. A similar correlation in band structure for bcc transition metals has been predicted by Mattheiss[33] from his band-structure calculations, but there is as yet little relevant experimental evidence.

[28] J. G. Hanus, MIT Report, 1962 (unpublished).
[29] E. Fawcett and W. A. Reed, Phys. Rev. **131**, 2463 (1963).
[30] J. C. Phillips, Phys. Rev. **133**, A1020 (1964).
[31] P. T. Coleridge, Phys. Letters **15**, 223 (1965).
[32] J. B. Ketterson, M. G. Priestley, and J. J. Vuillemin, Bull. Am. Phys. Soc. **10**, 1089 (1965).
[33] L. F. Mattheiss, Phys. Rev. **134**, A970 (1964).

It now remains to explain an apparent contradiction between the present data and conclusions drawn from a rigid-band model for Pd-Ag systems. Budworth *et al.*[6] have used their specific-heat data for Pd-Ag systems to show that Pd has approximately 0.58 holes/atom in the *d* bands, which is much larger than the present value of 0.36 even though both sets of data are based on the same model. This does not necessarily indicate an inconsistency in the rigid-band model as applied to alloys. These macroscopically homogeneous but random alloys have a binomial distribution of nearest neighbors of one kind.[34,35] The *d*-band states are determined largely by nearest-neighbor interactions in a tight-binding approximation and in these alloys the statistical fluctuations of the overlap integral must be taken into account. This seems to be a rather complex effect, but it is reasonable to suppose that observed quantities such as the density of states are in effect an average over a range of alloy concentrations. A rough estimate of this range shows that it gives approximately the correction needed to account for the discrepancy.

[34] I am indebted to Professor J. C. Phillips for the argument that follows.

[35] V. Jaccarino and L. R. Walker, Phys. Rev. Letters **15**, 258 (1965).

ACKNOWLEDGMENTS

I would like to thank Professor M. G. Priestley for his guidance, assistance, and keen interest in all phases of this work. The assistance of Professor R. W. Stark and L. R. Windmiller with the modulation technique and Dr. R. W. Johnson with the sample preparation is appreciated. I am grateful for theoretical discussions with Professor J. C. Phillips and F. Mueller and for permission to quote their results prior to publication.

PHYSICAL REVIEW VOLUME 144, NUMBER 2 15 APRIL 1966

Size-Effect Variation of the Optical Properties of Conductors

YI-HAN KAO

Department of Physics, State University of New York at Stony Brook, Stony Brook, New York

(Received 8 September 1965; revised manuscript received 19 November 1965)

The influence on the optical reflectivity and the complex index of refraction of thin conducting films, due to the variation of thickness and electronic mean free path, is investigated. The calculation is based upon Chambers' kinetic analysis. It is shown that, when the penetration depth exceeds the film thickness, with diffuse scattering of electrons at the boundaries, the resistivity is an oscillatory function of both frequency and thickness. Consequently, these oscillations will result in fluctuations in the optical reflectivity. The "optical-size effect," which is important in conducting films of thickness $\lesssim 10^{-5}$ cm, may give rise to pronounced changes in the characteristics of the frequency variation of the optical reflectivity.

I. INTRODUCTION

IT has been known for many years that a thin conductor exhibits a higher electrical resistivity than the bulk material if the thickness is smaller than the mean free path of the conduction electrons. Extensive studies of the "size effect" have been made in the past for conductors in a dc electric field, from which useful information on the electronic mean free path and other transport properties have been obtained.[1] The purpose of this paper is to discuss a case where a thin conductor is placed in an ac electric field and, consequently, in the high-frequency regions, the optical properties are size-dependent. Since measurements of the optical phenomena in conductors are sometimes made with thin films, it is worth noting that the size effect should be taken into account to determine the optical parameters when the conditions discussed below are satisfied.

[1] For a review of the size effect, see J. M. Ziman, *Electrons and Phonons* (Oxford University Press, London, 1960), Chap. XI.

Let us consider a thin conducting slab of thickness d. In a dc electric field, when d is large compared with the electron mean free path l in the conductor, the resistivity is essentially determined by the scattering process occurring in the bulk while the boundary effects can be neglected. In this case, the resistivity is independent of d. However, for thin specimens with $d<l$, as can be found in ordinary metals with $d\lesssim 10^{-5}$ cm at room temperature and $d\lesssim 10^{-2}$ cm at liquid-helium temperatures, scattering of electrons at the boundary surfaces actually limits the effective mean free path and plays an important role in determining the resistivity of the specimen. Indeed, the dc resistivity has been found as a monotonic function of d/l in many metals. Nevertheless, in an oscillating electric field of optical frequency ω impinging from one side of the specimen, the ac resistivity will essentially be determined by the "effective electrons" moving in the skin depth δ and traversing nearly parallel to the surface which receives the field. The size effect in this case will depend not only on d and l, but also on δ. The most favorable condition